Performance Analysis and Aerodynamic Design of Axial Flow Compressors

Saleh.B. Mohamed
Al-Zaituna University, Tarhoona, Libya
Saleh_ba2004@yahoo.com

Mohamed.H.El-Hasnawi
Al-Zaituna University, Tarhoona, Libya
Elhasnawi@gmail.com

Abstract—**The main objective of the paper is to analyze the performance of axial flow compressors and to generate a systematic design approach which enables to design subsonic flow ones. In order to investigate the validity of this approach, the LP axial flow compressor of the RR Spey MK511 turbofan engine is taken as an example. The design calculations were based on thermodynamics, gas dynamics, fluid mechanics and empirical relations. The flow is assumed to be of two-dimensional compressible type with constant axial and rotor blade velocities with a free-vortex swirl distribution. Design calculations include thermodynamic properties of the working fluid, number of compressor performance parameters such as, stage temperature rise and number, flow and blade angles (blade twist), velocity triangles and relative inlet Mach number at rotor blades tips as well as blades tip and hub diameters. A repeated calculation is made to determine these parameters along compressor stages. The variation of velocity whirl components, air and blade angles, deflection and degree of reaction from root to tip of the blades were also determined. The twist of the blades along the blade length is set according to the recommended values in order to obtain smooth blade twist profile.**

Index Terms: **LP compressor, stage, pressure ratio, performance, efficiency, velocity, reaction, factor, angle.**

I. INTRODUCTION

Axial flow compressor is one of the most common types of compressors. It finds its major application in large gas turbine engines like those powering today's jet aircrafts, it derives its name from the fact that the air being compressed has very little motion in the radial direction, in contrast, the radial motion of the air in centrifugal compressor is much longer than the axial motion. In general, the axial machines have much greater mass flow but much less pressure ratio per stage because of the boundary layer behavior, and fundamentally, the axial compressor is limited by boundary layer behavior in adverse (positive) pressures gradients [1,2] . It is made up of two major assemblies; the rotor with its blades and the casing with its stationary blades (stator) are making one stage as shown in Figure.1 [1,2,3].

Received 28 July 2016; revised 4 August 2016; accepted 23 September 2016.

Available online 24 September 2016.

The rotor increases the angular velocity of the fluid resulting increase in total temperature, total and static pressures.The following stator decreases the angular velocity of the fluid, resulting in an increase in the static pressure and sets the flow up for the following rotor.

The axial compressor may be designed with constant tip, mean and hub diameter or with all varying; however the mean blade radius does not usually change very much and thus preferred [2,3]. The blade length varies in order to accommodate the variation in air density so that the axial velocity component will be approximately uniform.

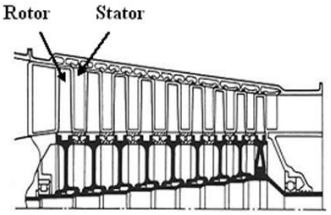

figure 1. An Axial Flow Compressor Stage

II. OVERVIEW OF RR SPEY MK 511 TURBOFAN ENGINE

Rolls Royce Spey MK 511 is a turbofan engine having two shafts with no distinct fan and airflow diverted from the LP compressor spool. By pass ratio is only 0.66. The LP compressor in task has 5 stages, with engine bleed used for anti-icing. The Hp compressor has 12 stages, with variable stators on the first stage, a 10 element annular combustion chamber, a two stage Hp turbine, with the first stage air cooled, a two stage LP turbine and a clamshell thrust reverser. There were no inlet guide vanes in front of the compressor. The maximum takeoff thrust of the engine is 50.6 KN. The LP compressor operating conditions are given in Table 1 [4].

Table 1. LP Compressor Operating Conditions

Specifications	
Type of compressor	**Constant mean diameter**
Mass flow rate	56.02 kg/s
Pressure ratio	2.565
Polytrophic efficiency	0.9
Inlet temperature	298.23 K
Inlet pressure	1.023 bar
Constant axial velocity	155 m/s

III. AXIAL FLOW COMPRESSOR MAIN PERFORMANCE PARAMETERS

A. Stage Velocity Diagram

The air should enter the compressor axially and should be deflected into a direction that matches the first stage rotor inlet as shown in Figure. 2. The air approaches the rotor with a velocity C_1 at an angle α_1 from the axial direction, combining C_1 vectorially with the blade speed U gives the velocity relative to the blade V_1 at a inlet blade angle β_1 from the axial direction. After passing through the rotor, the absolute velocity of the air is increased, the fluid leaves the rotor with a relative velocity V_2 at an outlet blade angle β_2 determined by the rotor blade outlet angle. Assuming that the design is such that the axial velocity C_a is kept constant, the value of V_2 can be obtained and the outlet velocity triangle constructed by combining V_2 and U vectorially to give C_2 at outlet air angle α_2. The air leaving the rotor at α_2 then passes to the stator where it is diffused to a velocity C_3 at outlet air angle α_3, and typically the design is such that $C_3 \approx C_1$ and $\alpha_3 \approx \alpha_1$ so that the air is prepared to enter another similar stage. Assuming that Ca= Ca1=Ca2 the following basic equations from the geometry of the velocity triangles shown in Fig.2 [1.2] can be deducted:

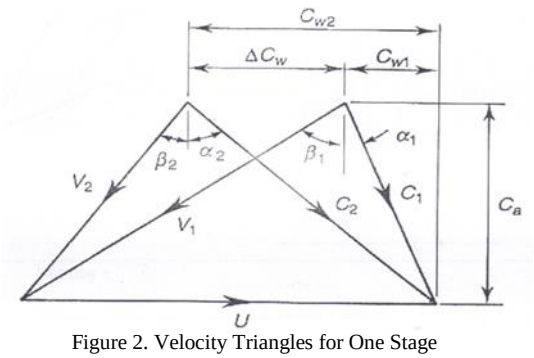

Figure 2. Velocity Triangles for One Stage

$$\frac{U}{Ca} = \tan\alpha_1 + \tan\beta_1 \qquad (1)$$

$$\frac{U}{Ca} = \tan\alpha_2 + \tan\beta_2 \qquad (2)$$

$$Cw_1 = C_a \tan\alpha_1 \qquad (3)$$

$$Cw_2 = C_a \tan\alpha_2 \qquad (4)$$

B. Compressor Stage Pressure Ratio

The compressor pressure rise is strongly dependent on the efficiency of the compression process which is given by [2, 3]:

$$\eta_{is} = \frac{T_{03}` - T_{01}}{T_{03} - T_{01}} \qquad (5)$$

The stage pressure ratio can be then given by [2,3]:

$$R_s = \frac{P_{03}}{P_{01}} = \left[1 + \eta_{is}\frac{\Delta T_{0s}}{T_{01}}\right]^{\frac{\gamma}{\gamma-1}} \qquad (6)$$

In order to obtain a high temperature rise in a stage, which is desirable to minimize the number of stages for a given overall pressure ratio, combination of high blade speed (U), high axial velocity (Ca) and high blade deflection (β_1-β_2) must be targeted in early design stages. But care should be taken since the blade stresses will obviously limit the blade speed, while adverse pressure gradient combine to limit high the target of high axial velocity and high deflection [2, 5, 6, 8]. Thus, the design is always a compromise between the conflicting requirements.

C. Compressor Multistage Pressure Ratio

The compressor multistage pressure ratio (R_c) can be determined on the basis of the temperature and pressure change for a single stage [2, 8]. The procedure requires then the calculation of such pressure and temperature change and to repeat these calculations for each stage until the required compressor overall pressure ratio is obtained. For compressors having identical stages, the stage efficiency can be considered as equal to the polytropic (η_p) efficiency for the reasons that the temperature rise of an axial compressor is small. Thus, in a compressor between any pair of stagnation state (01) and (02) for a constant η_p andγ, the overall pressure ratio can be given by:

$$R_c = \frac{P_{02}}{P_{01}} = \left(\frac{T_{02}}{T_{01}}\right)^{\frac{\gamma\eta_{poly}}{\gamma-1}} \qquad (7)$$

And for constant specific heats, the adiabatic compression efficiency is given by [2, 8]:

$$\eta_c = \frac{\left(\frac{P_{02}}{P_{01}}\right)^{\frac{\gamma-1}{\gamma}} - 1}{\frac{T_{02}}{T_{01}} - 1} \qquad (8)$$

The combination of equations 7 and 8 shows that the relationship between overall adiabatic and polytropic compression efficiencies depend on the overall pressure ratio, as follows [8, 9, 11]:

$$\eta_c = \frac{\left(\frac{P_{02}}{P_{01}}\right)^{\frac{\gamma-1}{\gamma}} - 1}{\left(\frac{P_{02}}{P_{01}}\right)^{\frac{\gamma-1}{\gamma\eta_{poly}}} - 1} \qquad (9)$$

D. Inlet Axial Flow Velocity

The inlet axial flow velocity effects the annulus dimensions required to pass the mass flow, and hence the overall size of the engine. A high inlet axial velocity is required to obtain high temperature rise per stage which is desirable to minimize the number of stages for a given overall pressure ratio [2, 9, 11, 13]. But this increases the adverse pressure gradient that increases the local boundary layers and losses.

In general, this parameter is dependent on the engine application. For industrial engines, the size is not critical and hence low value of inlet axial flow velocity can be tolerated. But for aero engines compactness is required and higher values of inlet axial flow velocity is targeted and up to 200 m/sec is permitted [2, 5, 8, 11]. For the current work a constant inlet axial velocity and as a good compromise between achieving a reasonable compressor efficiency and overall performance a value of 155 m/sec is selected.

E. Inlet and Outlet Hub-Tip Ratios

The inlet hub-tip ratio, in axial flow compressors varies normally between 0.4 and 0.6, while at the compressor outlet values as high as 0.92 maximum can be used [2, 5, 11, 14, 16]. Using low hub-tip ratio could result in a mismatch between compressor and turbine diameters and may also complicate both the mechanical and aerodynamic design for the first stage, while, using high inlet hub-tip ratio increases the compressor diameter and weight.

F. Compressor Work

The flow enters the compressor rotor at radius r_1 and leaves at r_2 as shown in Figure. 3. Therefore the work per unit mass W_c done on the fluid by the rotor is:

$$W_c = U(C_{w2} - C_{w1}) = U\,\Delta C_w \qquad (10)$$

By assuming an adiabatic process and from the T-s diagram of a typical compressor stage shown in Figure. 4, the input work to the compressor can be determined by the following expression:

$$W_c = C_p(T_{02} - T_{01}) \qquad (11)$$

Equations 10 and 11 yield,

$$\Delta T_0 = \frac{U\Delta C_w}{C_p} \qquad (12)$$

Referring to the stage velocity diagram shown in Figures. 3 and 4 and accounting for work done factor we get,

$$\Delta T_{0s} = \frac{\lambda U C_a}{C_p}(\tan\beta_1 - \tan\beta_2) \qquad (13)$$

Where, $\Delta T_{0S} = T_{03} - T_{01} = T_{02} - T_{01}$

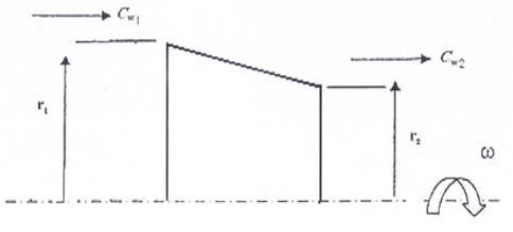

Figure 3. Flow Entering a Rotor of an Axial Flow Compressor

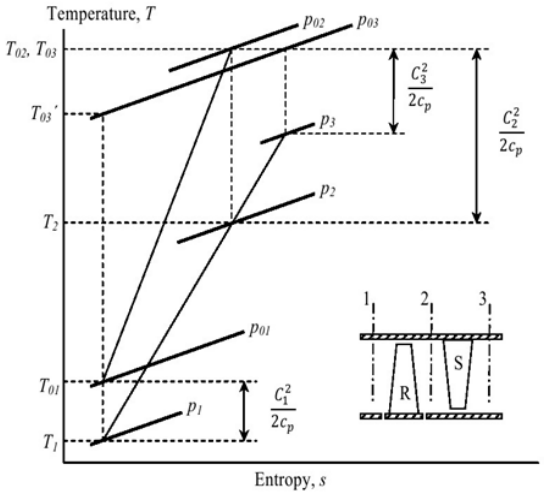

Figure 4. Compressor Stage and Velocity Diagram

G. Flow Coefficient (φ)

The flow coefficient is defined as:

$$\varphi = \frac{C_a}{U} \qquad (14)$$

If the blade speed is held constant, an increase in the flow coefficient will result in an increase of air entrance blade angle β_1. The recommended typical values for flow coefficient are in the range of 0.3 to 0.6.

H. Stage Loading (Ø)

The stage loading is defined as the ratio of the actual enthalpy rise in the stage to the square of blade speed [1, 2, 3, 8]. Thus,

$$\emptyset = \frac{W_c}{U^2} = \frac{C_P\Delta T_0}{U^2} = 1 - \frac{C_a}{U}(\tan\alpha_1 + \tan\beta_2) \qquad (15)$$

The stage loading is a criterion of the limitations imposed by blade velocity on the work done on the air in the stage. The recommended typical values for the stage are between 0.3 and 0.5.

I. Diffusion Factor

Diffusion takes place through both rotor and stator blades and a diffusion factor is used to access its amount. This factor relates empirically the peak velocity on the suction surface of the blade to the velocity at the trailing edge [1, 2, 3, 9].

$$DF = 1 - \frac{V_2}{V_1} + \frac{\Delta V_w}{2\,V_1}\left(\frac{S}{C}\right) \qquad (16)$$

Factors less than 0.4 for the blade tip and less than 0.6 for the blade root are usually taken as typical recommended values at the design point.

J. Stage Reaction

The stage reaction (R) is defined as the fraction of the rise in static enthalpy in rotor compared to the rise in stagnation enthalpy throughout the entire stage [1, 2].

Many expressions are available to determine the stages of reaction among these are:

$$R = \frac{C_a}{2U}(\tan\beta_1 + \tan\beta_2) \qquad (17)$$

If a compressor stage would have a stage reaction of 1.0 or 100%, the rotor would do all of the diffusion in the stage. Similar, if the stage reaction is 0 than the stator will do all of the diffusion of the working fluid. It is never good to have either a stage reaction of 1.0 or 0. The suggested stage reaction in literature is about 0.5 i.e. the diffusion is equally divided between the two blade rows. But in practice a higher stage reaction is preferred in order to decrease in whirl prior to the rotor, as smaller whirl will create a larger relative inlet velocity to the rotor row, at a constant C_p, and hence make it easier for the rotor to increase the static pressure.

K. De-Haller Number

In most compressor stages both the rotors and the stators are designed to diffuse the fluid, and hence transform its kinetic energy into an increase in static enthalpy and static pressure. The more the fluid is decelerated, the bigger is the pressure rise, but boundary layer growth and wall stall are always is limiting this process. To avoid this, de-Haller proposed that the overall deceleration ratio, i.e. V_2/V_1 and C_2/C_3 in a rotor and stator respectively, should not be less than 0.72 (historic limit) in any row [1, 2, 3].

$$DH = \frac{V_2}{V_1} \geq 0.72 \qquad (18)$$

L. Work Done Factor

The energy input to the fluid will be absorbed usefully in raising the pressure and velocity of the air and some will be wasted in overcoming various frictional losses. However, the whole of the work input will appear as a stagnation temperature rise of the air regardless of the isentropic efficiency. In practice the flow inlet axial velocity (C_a) is not constant along the length of the blade, and to account for this, a work done factor λ is introduced and defined as [1, 2, 3]:

$$\lambda = \frac{(T_{03} - T_{01})}{U\,C_a(\tan\beta_1 - \tan\beta_2)/C_P} \qquad (19)$$

The variation of work done factor shown in Figure 5 indicates that λ decreases as the number of compressor stages increases. Typical stages work done factor are listed in Table 2.

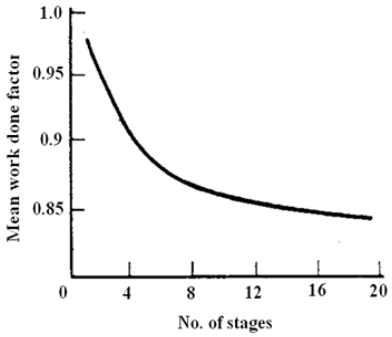

Figure 5. Variation of mean work done factor with number of stages

Table 2. Typical Values of Work Done Factor

Stage No.	Work done factor	Degree of reaction (*R*)
1	0.98	0.86
2	0.93	0.7
3	0.88	0.5
4	0.83	0.5
5	0.83	0.5

M. Compressor Isentropic Efficiency

Compressor isentropic efficiency is directly proportional to the compressor pressure ratio and inversely proportional to its discharge temperature. The following equation more exactly defines the compressor isentropic efficiency [1, 2, 3, 5, 12]:

$$\eta_{is} = \frac{R_c^{\frac{\gamma-1}{\gamma}} - 1}{\frac{T_0}{T_1} - 1} \qquad (20)$$

IV. DESIGN METHOD

The design point choice is made; to satisfy engine design requirements of high mass flow rate and minimum structural weight and to take into considerations the design constraints that avoid an excessive blade twist. These constraints are related to de-Haller number, flow coefficient, stage loading, axial flow velocity (C_a) and hub to tip ratio (r_h/r_t). Thus, an axial velocity (C_a) and hub to tip ratio (r_h/r_t) 155 m/sec and 0.5 are selected respectively to perform the design point calculations. The design input data was summarized in Table 1.

A. Determination of Rotational Speed and Annulus Dimensions

There is no equation which enables the designer to select a suitable value of rotational speed. Instead, it can be found by assuming values for blade tip speed, axial flow velocity and hub to tip ratio for the first stage, while the required annulus area at inlet can be found from the specified air mass flow rate, assumed flow axial velocity and flow ambient conditions.

The suggested tip speed (U_t) found in literature that promises acceptable stress values is in the order of 350 m/sec. Without an IGV there will be no whirl component of velocity at inlet and this will increase the flow Mach number relative to the blade, as shown in Fig. 6.

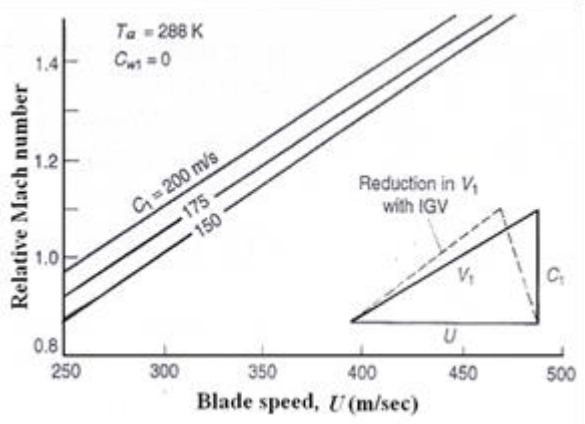

Figure 6. Relative Mach Number at Rotor Entry

The annulus cross sectional area for the flow at inlet can be then expressed as:

$$A_1 = \pi r_t^2 \left(1 - \left(\frac{r_r}{r_t}\right)^2\right) \qquad (21)$$

To satisfy the continuity equation:

$$\dot{m} = \rho\pi r_t^2 \left[1 - \left(\frac{r_r}{r_t}\right)^2\right] C_a \qquad (22)$$

$$r_t = \sqrt{\frac{\dot{m}}{\rho\pi C_a \rho\pi \left[1 - \left(\frac{r_r}{r_t}\right)^2\right]}} \qquad (23)$$

From the LP compressor operating conditions listed in Table1, T_{01}=298.229K, P_{01}=1.023 bar with C_a =155m/sec, C_{w1}=0, we get the static temperature and pressure as well as the flow density at the compressor inlet, T_1=286.216 K, P_1=0.8864 bar, ρ_1=1.0789 kg/m3, respectively.

A selected geometry of blade hub to tip ratio (r_r/r_t) of 0.5 is considered to promise a merely sensible starting point for this simple engine, and with the inlet flow properties calculated above, the tip radius (r_t) of the blade = 0.485824m. Then it follows that the blade root radius (r_h) = 0.2429m and the mean radius (r_m) = 0.3644m, while inlet annulus area (A_1) = 0.5506 m^2. The blade height (h_1) can be then found by:

$$h_1 = \frac{A_1}{2\,\pi\, r_m}$$

The blade tip speed is related to the radius of the blade at the tip (r_t) by U_t=2π r_tN, and as U_t is selected 350 m/sec, then the number of revolutions (N) can be found easily as 114.66 rev/sec.

The relative Mach number at the inlet of the compressor rotor tip (M_{1t}) can be found by assuming a constant annulus axial velocity (which is the case with no inlet guide vanes) as follows:

$$V_{1t} = \sqrt{U_{1t}^2 + C_{a1}^2}$$

$$M_{1t} = \frac{V_{1t}}{\sqrt{\gamma R T_1}}$$

The compressor delivery pressure (P_{02}) = 2.565 x 1.023 =2.624 bar and on the basis of estimated polytropic efficiency (η_{poly}) of 0.9, the delivery temperature can be estimated by using equation 7 above and found equals 402.183K. In turn, the static flow properties (pressure, temperature and density) at the compressor exit can be found by assuming the air leaving the stator of the last stage with an axial velocity of 155 m/sec and with no whirl and by using the Isentropic relations found in references [1,2,3] as T_2=390.224K, P_2=2.361*bar*, respectively. In turn, the exit flow density is 2.108 *kg/m*^{3}.

The exit annulus area (A_2) can be then given by the continuity equation and found equals 0.2846 *m*^{2}.

With the blade mean radius (r_m) of 0.3644m, the blade height (h_2) on exit is given by:

$$h_2 = \frac{A_2}{2\,\pi\, r_m}$$

The blade radii at the exit from the last stator of the compressor stage are then:

$$r_t = r_m + \frac{h_2}{2}$$

$$r_r = r_m - \frac{h_2}{2}$$

B. Estimation of Number of Stages

With the assumed polytropic efficiency (η_{poly}) of 0.9, the overall stagnation temperature rise through the compressor is 402.183-298.229=103.954K. The stage temperature rise ΔT_{0s} can vary widely in different compressor designs, depending on the application and the importance or otherwise low weight. Values may vary from 10 to 30K for subsonic stages and may be 45K or higher for high transonic stages. Rather than choosing a value randomly, it is instructive to estimate a suitable ΔT_{0s} based on the mean blade speed. Since a simple design condition of constant axial flow velocity is selected i.e. C_{a1}=C_{a2}=....=C_a=155 m/sec, then the mean blade speed can be found as follows:

$$U_m = 2\pi r_m N = 262.524\ m/sec$$

Then the stage temperature rise can be found by using equations 12 and 13 above. With purely axial velocity at entry to the first stage, in the absence of IGV, The flow angle at entry (α_1) equals 0. Thus, from equation 1, the rotor blade inlet angle (β_1) equals 59.44^o.

The rotor relative inlet velocity (V_1) can be then found from equation 1 and found equals 304,854 *m/sec*.

In order to estimate the maximum airflow deflection in the rotor, The De Haller number criterion discussed above is employed, and by considering a De-Haller number (V_2/V_1) of 0.72, the rotor relative inlet velocity (V_2) equals can be then found 219.5 m/sec. The

corresponding rotor blade outlet angle can be then found from equation 2 and found equals 45.08°.

By using this deflection and neglecting the work done factor for this crude estimate, the stage temperature rise is found by using equation 13 above as 25.173*K*. This temperature rise implies 103.954/25.173 = 4.13 stages. It is likely, then, that the compressor will require five stages. With five stages and an overall temperature rise 103.954K, the average temperature rise per stage is 20.79K. It is then recommended to design to somewhat lower temperature rise in the first and last stages. A good starting point would be to assume $\Delta T_0 \approx 18K$ for the first and last stages, leaving a requirement for $\Delta T_0 \approx 24K$ in the third stage and $\Delta T_0 \approx 22K$ for the fourth and fifth stages, as shown in Table 3.

Table 3. Temperature Rise for Each Stage

Stage No.	$\Delta T_0(K)$
1	18
2	22
3	24
4	22
5	18

C. Stage by Stage Design

Having determined the rotational speed, annulus dimensions and the required number of stages, the next step is to evaluate the air angles for each stage and at the mean radius. A step is required to check if the estimated number of stages is likely to result in an acceptable design. From the velocity diagram shown in Figure. 2, it can be seen that $C_{w1}=C_a \tan\alpha_1$ and $C_{w2}=C_{w1}+\Delta C_w$. For the first stage $\alpha_1=0$, as these is no inlet guide vane. The stator outlet angle for each stage α_3 will be the inlet angle α_1 or the following rotor. Calculations of stage temperature rise are based on rotor considerations only, but keeping reasonable level of diffusion in the stator should be considered. The work done factor (λ) and the degree of reaction (R) will vary through the compressor and reasonable values for the five stages found in literature are shown in Table 2 above.

A. Stages 1 and 2

Recalling for the equation for the stage temperature rise in change of flow whirl velocity, $\Delta C_w=C_{w2}-C_{w1}$, we have from equation 12 above, we get $\Delta C_w=70.28$ *m/sec*.Since $C_{w1}=0$, then $C_{w2}=\Delta C_w=70.28$ *m/sec*. The first stage rotor blade inlet angle β_1 was already found and equal 59.44°, thus, the outlet blade angle $\beta_2$from the stage is given by equation 2 and found 51.12°.

Also, the outlet flow angle from the first stage (α_2) can be given from equation 2 and found 24.39°.

The velocity diagram for the first stage is shown in Figure 7 (a). For this stage, the deflection in the rotor blades is 8.32° ($\theta = \beta_1-\beta_2$), which is modest. The diffusion can be reality be checked using the de-Haller number as (V_2/V_1) which is 0.81. This value indicates a relatively light aerodynamic loading, i.e. a low diffusion rate. The first stage pressure ratio denoted as $(P_{03}/P_{01})_1$ is found by using equation 6 and by assuming that the isentropic and polytropic efficiencies for this stage are equal, thus $(P_{03}/P_{01})_1$ equals 1.2038.

Then the stage outlet stagnation pressure $(P_{03})_1$ and temperature $(T_{03})_1$ are 1.2315 bar and 316.23K. Also the stage degree of reaction can be given by using equation 17 and found equals 0.866.

Finally we have to choose a value for the flow air angle at the stator row outlet (α_3), that will in direction with the rotor inlet flow angle (α_1) into the second stage. For the second stagewe have the stage temperature rise (ΔT_0) is 22K, the work done factor (λ) is 0.93. The degree of reaction (R) for this stage should be selected arbitrary making an attempt to achieve 50 percent in the later stages, thus a 70 percent degree of reaction promises a good start. Equations 13 and 17 are then used to determine the rotor blade inlet (β_1) and outlet (β_2) angles. From equation 13 we get $(\tan\beta_1 - \tan\beta_2) = 0.583967$. From equation 17 we can get also $(\tan\beta_1 + \tan\beta_2) = 2.3711$. Solving these simultaneously we get, β_1=55.91° and β2=41.78°. By using equations (1) and (2) the flow angles at rotor inlet (α_1) and at rotor outlet (α_2) are 12.19° and 38.67°, simultaneously.

The whirl component of velocities at inlet (C_{w1}) and outlet (C_{w2}) for the rotor of this stage can be obtained from the velocity triangles shown in Fig. 2 and equation 3, and found equals 124.045 *m/sec*.

The required change in whirl velocity is $(\Delta C_w)_2$ = 90.56 *m/sec* is higher than $(\Delta C_w)_1$ (70.28 *m/sec* for the first stage), this is due to higher stage temperature rise and lower work done factor. The fluid deflection in the rotor blades has increased also to $(\theta)_2 = \beta_1-\beta_2$=14.13°.

Thus, it appears that the flow angle (α_3) for the first stage should be 12.19°. This design gives a de-Haller number for the second stage of a value equals to Cos (55.91)/Cos (41.78) = 0.752, which is satisfactory. The velocity diagram of the second stage is shown in Fig.7 (b), while the stage pressure ratio is determined by using the Isentropic relations found in references [1,2,3] which gives $(P_{03}/P_{01})_2$ of 1.2366.

Then the second stage outlet stagnation pressure $(P_{03})_2$ and temperature $(T_{03})_2$ are 1.52308 bar and 338.38K, respectively. At this point we do not know the flow angle at the stator outlet of this stage (α_3) , but it can be determined from the fact that it is equal to the flow angle at the rotor inlet (α_1) for the third stage, which will now proceed to consider. It is useful to point out that the degree of reaction is directly related to the shape of the velocity diagram. Also, it was previously shown that for 50% reaction, the velocity diagram is symmetric. Writing:

$$C_{wm} = ((C_{w1} + C_{w2})/2) \qquad (24)$$

$$R = 1 - \left({}^{C_{wm}}/_{U_m}\right) \qquad (25)$$

Referring to Figures 7 (a) and 7 (b), it can be seen that when (C_{wm} / U_m) is small (i.e. $3x10^{-4}$), and the corresponding reaction is high, then the velocity diagram is highly skewed; the high the degree of reaction in the first stage is a direct consequence of the decision to dispense with inlet guide vanes and use purely axial inlet velocity. The degree of reaction is reduced in the second stage, and this would be essentially liked to achieve 50% in the later stages where the hub-tip ratios are higher.

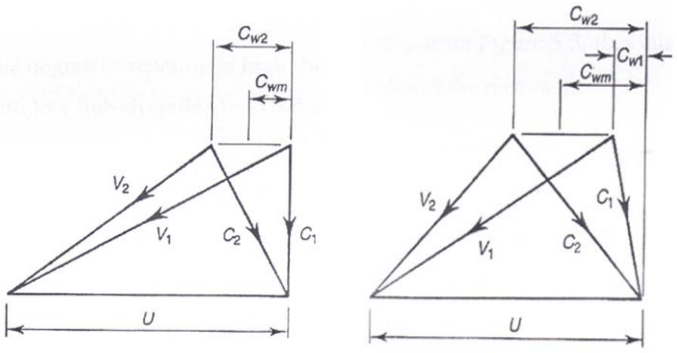

a) First stage b) Second stage

Figure 7– Effect of Degree of Reaction on the Shape of the Velocity

B. Stage 3

For the third stage, using a stage temperature rise of 24K and a work done factor (λ) of 0.88 with an attempt made to design the blades with 50% degree of reaction. Proceeding with the design calculations as before we get by using equation 13 $(\tan\beta_1 - \tan\beta_2) = 0.67$. Equation 17 gives also $(\tan\beta_1 + \tan\beta_2) = 1.6937$.

Solving the above two equations yields, β_1= 49.8^o and β_2= 27.03^o. The corresponding value of de Haller number is given V_2 / V_1 = 0.725 (i.e. Cos (49.8)/Cos (27.03), which is satisfactory.

The stage pressure ratio is $(P_{03}/P_{01})_3$ is 1.2418.

Then the third stage outlet stagnation pressure $(P_{03})_3$ and temperature $(T_{03})_3$ are 1.89138bar and 362.46K, respectively. From the symmetry of the velocity diagram shown in Fig.2, $\beta_1 = \alpha_2$= 49.8^o and $\beta_2 = \alpha_1$=27.03^o. Then the whirl velocities $(C_{w1})_3$ and $(C_{w2})_3$ can be given by equations 3 and 4 and found equals 79.08 *m./sec* and 183.42 *m/sec*, respectively.

C. Stages 4 and 5

For the last stages a work done factor (λ) of 0.83 and this is considered as appropriate for all stages from the fourth stage onwards, and a 50 percent degree of reaction (R) is used, while the design can be simplified by using the same velocity diagrams used earlier for the first stages, although each blade will have a different length due to continuous increase in density. The temperature rise (ΔT_0) for the fourth stage is 22, thus preceding with the design calculations as before we get, β_1= 49.47^o and β_2= 27.26^o. The corresponding value of de Haller number is given V_2 / V_1 = 0.731 (i.e. Cos (49.47)/Cos (27.26), which is satisfactory. Then the fourth stage outlet stagnation pressure $(P_{03})_4$ and temperature $(T_{03})_4$ are 2.278 bar and 384.525K, respectively. Also, from the symmetry of the velocity diagram shown in Figure. 3 and 4, $\beta_1 = \alpha_2$= 49.8^o and $\beta_2 = \alpha_1$=27.03^o. Then the whirl velocities C_{w1}, C_{w2} are 79.864 m/sec and 181.29, respectively. The temperature rise for the fifth stage (ΔT_0) is 18 and thus preceding with the design calculations as before yields, β_1= 48.1^o and β_2= 30.078^o. While the corresponding value of de Haller number is given V_2 / V_1 = 0.771 (i.e. Cos (48.1)/Cos (30.078), which is satisfactory. Then the stage outlet stagnation pressure $(P_{03})_5$ and temperature $(T_{03})_5$ are 2.632 bar and 402.56K, respectively. From the symmetry of the velocity diagram, $\beta_1 = \alpha_2$= 48.1^o and $\beta_2 = \alpha_1$=30.078^o. The whirl velocities C_{w1}, C_{w2} are 89.77 m/sec and 172.75 respectively. The design calculation results for the five stages are summarized in Table 4.

It is worth to notice that with a 50 percent degree of reaction used in the final stage, the flow will leave the last stage with an angle $\alpha_3 = \alpha_1$ =30.078^o whereas ideally the flow should be axial at entry to the HP compressor. Thus, the flow should be then straightened by incorporating vanes downstream the fifth stage of the LP compressor.

Table 4. Stages performance

Stage No.	**1**	**2**	**3**	**4**	**5**
P_{01}, bar	1.023	1.232	1.5231	1.8914	2.278
T_{01}, K	298.23	316.31	338.38	362.46	384.525
P_{03}, bar	1.232	1.5231	1.8914	2.278	2.632
T_{03}, K	316.31	338.38	362.46	384.525	402.56
(P_{03}/ P_{01})	1.204	1.2368	1.2418	1.2046	1.15538
α_1	0^o	12.19^o	27.03^o	27.26^o	30.078^o
α_2	24.39^o	38.7^o	49.8^o	49.47^o	48.1^o
β_1	59.44^o	55.91^o	49.8^o	49.47^o	48.1^o
$\beta 2$	51.12^o	41.78^o	27.03^o	27.26^o	30.078^o
R	0.866	0.7	0.5	0.5	0.5
De-Haller No.	0.81	0.752	0.725	0.731	0.771

V. VARIATION OF AIR AND BLADE ANGLES FROM ROOT TO TIP

The first stage is considered as a special case because of the axial inlet velocity and the third stage which is typical of the later stages due to the higher temperature rise. The variation of air angles from root to tip for the first stage will be investigated using free vortex design noting that the condition (C_{wr}) = constant is satisfied for C_w =0. Attention will be then turned to the design of the third stage, recalling that the design at the mean radius was based on stage degree of reaction (R_m) = 0.5. The third stage will be also investigated for the free vortex approach with R_m = 0.5. Considering the first stage, the rotor blade angle at inlet (β_1) is obtained directly from the

axial velocity (C_a) and the blade speed (U) at root, mean and tip. Thus for the free vortex condition we have:

$$(C_w r)_r = (C_w r)_m \dots\dots\dots\dots \therefore (C_w r)_r \left(\frac{r_m}{r_r}\right) \qquad (26)$$

$$(C_w r)_t = (C_w r)_m \dots\dots\dots\dots \therefore (C_w r)_t \left(\frac{r_m}{r_t}\right) \qquad (27)$$

At inlet: At outlet:

$$(\tan\alpha_1)_r = \frac{(C_{w1})_r}{C_a} \qquad (\tan\alpha_2)_r = \frac{(C_{w2})_r}{C_a}$$

$$(\tan\alpha_1)_m = \frac{(C_{w1})_m}{C_a} \qquad (\tan\alpha_2)_m = \frac{(C_{w2})_m}{C_a}$$

$$(\tan\alpha_1)_t = \frac{(C_{w1})_t}{C_a} \qquad (\tan\alpha_2)_t = \frac{(C_{w2})_t}{C_a}$$

$$(\tan\beta_1)_r = \left(\frac{U_r}{C_a}\right) - (\tan\alpha_1)_r \qquad (\tan\beta_2)_r = \left(\frac{U_r}{C_a}\right) - (\tan\alpha_2)_r$$

$$(\tan\beta_1)_m = \left(\frac{U_m}{C_a}\right) - (\tan\alpha_1)_m \qquad (\tan\beta_2)_m = \left(\frac{U_m}{C_a}\right) - (\tan\alpha_2)_m$$

$$(\tan\beta_1)_t = \left(\frac{U_t}{C_a}\right) - (\tan\alpha_1)_t \qquad (\tan\beta_2)_t = \left(\frac{U_t}{C_a}\right) - (\tan\alpha_2)_t$$

The variation of velocity whirl components, air and blade angles, deflection and degree of reaction from root to tip for the first and third stages are listed in Tables 5 and 6, respectively. The radial variation of air angles is shown in Figure.8 below. The degree of reaction at the root can be approximated by equation 17 because $C_1 \neq C_3$. And this gives:

$$R_r = 1 - \frac{155}{2x175.82}(\tan 34.22 + \tan 0) = 0.7$$

Table 5. Variation of air angles for first stage

	Root	Mean	Tip
C_{w1},m/sec	105.6	79.08	63.22
α_1	34.27°	27.03°	22.19°
β_1	30.44°	49.8°	59.7°
C_{w2},m/sec	244.83	183.42	146.64
α_2	57.66°	49.8°	43.39°
$\beta 2$	-18°	27.03°	49.55°
θ	48.44°	22.77°	10.15 °
R	0.104	0.5	0.68

Table 6. Variation of air angles for third stage

	Root	Mean	Tip
C_{w1},m/sec	0	0	0
α_1	0	0	0
β_1	48.47°	59.44°	66.04°
C_{w2},m/sec	105.43	70.28	52.72
α_2	34.22°	24.39°	18.78°
$\beta 2$	24.18°	51.12°	62.367°
θ	24.29°	8.32°	3.67 °
R	0.7	0.86	0.924

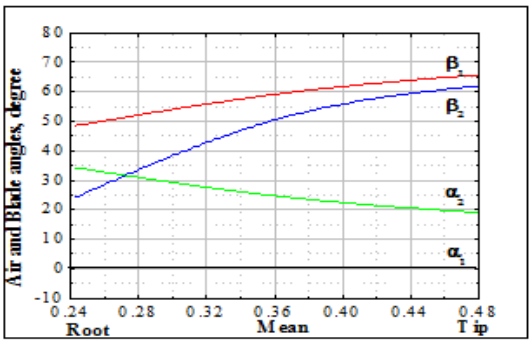

Figure 9. Radial Variation of Air and Flow Angles 1st Stage

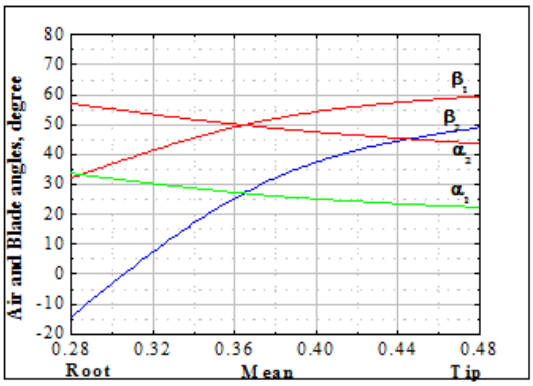

Figure 10. Radial Variation of Air and Flow Angles 3td Stage

As expected, with the high value of stage reaction (R_m) at the mean radius of 0.86 the problem with too low degree of reaction at root is avoided. The radial variation of the air angles for the third stage is shown in Fig.10 clearly indicates the very large fluid deflection ($\theta = \beta_1 - \beta_2$) required at the root and the substantial blade twist from root to tip. It is irrespective to consider a constant reaction design, with radial equilibrium ignored. With stage degree of reaction at the mean radius (R_m) =0.5, conditions at the mean radius will be the same as those previously considered for the free vortex design. As expected in the early design stages, a 50 percent stage degree gives symmetrical velocity diagram and this will hold across the annulus.

VI. CONCLUSIONS

A basic analysis of the performance of axial flow compressors is given and a methodical design approach is provided. The design calculations were performed using the recommended nowadays optimum starting design values found in literature. These include optimum values of axial flow velocity, blades hub to tip ratio, rotational speed, blades degree of reaction, stage work done factor, stage loading, diffusion factor, De-Haller number, stage temperature rise and relative inlet flow Mach number at the blades tips. The end result of the design calculations shows that five stages were necessary in order for the compressor to perform its duty. This matches exactly the number of stages of the existing engine compressor. However, other performance data could not be found for comparison since the MK511 turbofan engine is a

commercial engine in service and all original design data is a copyright of the manufacturer.

It is worth to mention that a degree of reaction for the first stage stages of 0.866 is high, but this is necessary in order to avoid a negative value at the root radius with low hub to tip ratios. Also the radial variation of air angles shown in Fig.8 indicated both the increased deflection ($\theta = \beta_1$-β_2) at the root and the requirement for considerable blade twist along the height of the blade which ensures that the blade angles are in agreement with the air angles and thus introducing incidence angles for each stage is vital. Thus, the design process must compromise between all conflicting requirements and design constraints.

VII. NOTATION

- η_{poly} Polytropic efficiency
- η_{is} Isentropic efficiency
- N Rotational speed, rev/sec
- U Blade speed, m/sec
- r Radius, m
- M Mach number
- h Blade height
- W Work, Watts
- C Whirl velocity, m/sec
- γ Specific heat ratio =1.4
- C_P Specific heat at constant pressure = 1004.5 KJ/Kg.K
- β Blade angle, degree
- α Flow angle, degree
- θ Flow deflection (β_1-β_2)
- IGV Inlet guide vane
- DF Diffusion factor
- λ Work done factor
- V Flow relative speed, m/sec
- φ Flow coefficient
- $\emptyset$ Stage loading
- DH De-Haller number
- S/C Space to chord ratio
- ΔT_0 Stagnation temperature rise, K
- ρ Flow density, kg/m^3
- T Static temperature, K
- P Static pressure, bar
- T_0 Stagnation temperature, K
- P_0 Stagnation pressure, Bar
- R_c Pressure ratio
- R Degree of reaction

Suffixes

- 1 Inlet
- 2 Outlet
- a Ambient, axial
- t Tip
- r Root
- m Mean
- 0 Stagnation
- 1,2,3 etc Reference planes
- c Compressor
- *w* Whirl

REFERENCES

[1] Bathic, William. "*Fundamentals of Gas Turbines*". Jhon Wiley & Sons, Inc, Second Edition, 1996.

[2] Cohen H., Rogers G.F.C.,&Hill Saravanamuttio H.L.H."'*Gas Turbine Theory*". Longman Group limited, Burt Harlow, Essex, U.K. 4th edition, 1996.

[3] Hill and Peterson *"Mechanics and Thermodynamics of propulsion*", 2nd, Addison-Wesley Publishibg, Inc. USA, 1992.

[4] Rolls-Royce Spey, "*World Encyclopedia of Aero Engines - 5th edition*" by Bill Gunston, Sutton Publishing, 2006, p.197.

[5] Niclas Falck "*Axial Flow Compressor Mean Line Design*", Thermal Power Engineering, Energy Sources, Lund University, Sweden, February 2008.

[6] B.B.Raval & V.G.Virani "*Aerodynamic Design of Axial Flow Compressor*", IJEDR, Volume 2, Issue 1 , ISSN: 2321-9939, 2014.

[7] Gaddam Srikanth Ȧ, S.Srinivas Prasad , V.Mahesh Kumar Ȧ and B.Mounica Reddy "*Design Methodology of a Two Stage Axial Compressor*", International Journal of Current Engineering and Technology, E-ISSN 2277 – 4106, P-ISSN 2347 – 5161, 2014.

[8] Meherwan P. Boyce, "*Gas turbine Engineering Handbook*", Gulf Professional Publishing, third Edition, 2006.

[9] Ronald H Aungier, "*Axial Flow Compressor: A strategy for Aerodynamic Design and Analysis*".Wiley Publication, ISBN: 978-1-86058-422-0, May 2003.

[10] Akin Keskin "*Application of multi-objective optimization to axial compressor preliminary design*" Aerospace Science and Technology 10 (2006) 581–589.

[11] Fengrui Sun "*Optimum design of a subsonic axial flow compressor stage*" Applied Energy 80 (2005) 187–195.

[12] B.T. Lebele-Alawa, "*Rotor-blades*" profile influence on a gas-turbines compressor effectiveness", Applied Energy 85 (2008). Pp.494–505.

[13] X.C. Zhu, "*The Off-Design Performance Prediction of Axial Compressor Based on A 2d Approach*" .Journal Of Theoretical and Applied Mechanics 51, 3, (2013). Pp. 523-531.

[14] Wall R. Axial-flow compressor performance prediction. AGARD-LS-83 1976(June):41–434.

[15] Calvert WJ, Ginder RB. Transonic fan and compressor design. Proc Instn Mech Engrs1999;213(C5):419–36.

[16] Gallimore SJ. Axial-flow compressor design. Proc Instn Mech Engrs 1999;213(C5):437–49.

[17] Egorov IN., "*Optimization of multi-stage axial compressor in a gas-turbine engine system*". ASME paper, 92-GT-424 1992.

[18] N. Cumpsty, "*Compressor Aerodynamics*", Krieger Publishing Company,2004.